Available online at www.sciencedirect.com

SciVerse ScienceDirect

Energy Procedia 29 (2012) 166 – 176

Energy Procedia

World Hydrogen Energy Conference 2012

Modelling and Performance of a Microtubular YSZ-based Anode Supported Solid Oxide Fuel Cell Stack and Power Module.

A. M. Ferriz[a]*, M. A. Laguna-Bercero[b], M. Ruperez[a], J. Mora[a], L.C. Correas[a]

[a]*Foundation for the Development of new hydrogen technologies in Aragon, Walqa Technology Park, Ctra. Zaragoza N330A, km566, E – 22.197 Huesca (S pain)*

[b]*Material Science Institute in Aragon, University of Zaragoza, 12, Pedro Cerbuna St., E – 50.009, Zaragoza (Spain)*

Abstract

The integration feasibility of the stack in a portable power module is demonstrated by the conceptual design of the system. An energy balance is simulated with Matlab Simulink®. The operation modes of the system, efficiency and convection inside the stack are studied via the Simulink® simulation. Also an electrical simulation is done for the complete cell characterization. A modular 3D design of the stack is also drawn using Solid Works®. The model will be validated with the fabrication of an experimental microtubular cell stack. An experimental 2cell-stack has been built and tested with a total power of 0.9W.

Keywords: Microtubular, SOFC, anode-supported, stack.

1. Introduction

Solid Oxide Fuel Cells (SOFC) are probably the most efficiency devices for the chemical energy conversion into electrical energy. Those systems are particularly attractive due to their high thermodynamic efficiency, fuel flexibility and zero emission. In terms of SOFC designs, there are traditionally two types of systems based on their geometry: planar and tubular. The advantages and disadvantages of both designs have been widely discussed [1]. The main advantages of tubular cells of tubular cells are higher mechanical and thermal stability and simpler sealing requirements, whereas planar designs are preferred in terms of high power density, high efficiency and low manufacturing costs. In the recent years, there has been an increasing interest in reducing the diameter of tubular SOFCs. The

* Corresponding author. Tel.: +34.974.215.258; fax: +34.974.215.261.
E-mail address: aferriz@hidrogenoaragon.org (A.M.Ferriz).

1876-6102 © 2012 Published by Elsevier Ltd. Selection and/or peer-review under responsibility of Canadian Hydrogen and Fuel Cell Association.
Open access under CC BY-NC-ND license. doi:10.1016/j.egypro.2012.09.021

microtubular SOFC design is preferred, especially for portable applications, due to their improved advantages such as: higher power densities per volume unit, rapid start-up/shut-down and higher durability under thermal stresses and redox cycles when we compared with planar and tubular conventional designs [2, 3, 4, 5, 6, 7, 8, 9]. Relevant studies in terms of thermal stability, redox-cycling and long-term testing can be found in references [10, 11, 12, 13].

The use of modelling for microtubular SOFC devices has also attracted great interest. Computational modeling is in this field complex due to the high number of physical processes involved such as mass and heat transfer, electrochemical reactions, molecular interactions or fluid dynamics. Most important aspects regarding computational modeling are summarized in the review of Lawlor *et al.* [6]. For example, Lockett *et al.* [14] performed Computational fluid dynamics (CFD) simulations of a single microtubular cell in order to predict temperature profiles for scale up of a 20-cell microtubular SOFC stacks. They found that the variation of temperature along the microtubes is a potential problem for the performance of the cell. Watanabe *et al.* [15] designed a thermal self-supported 700 W-microtubular stack using LSGM based cells. They found that their SOFC module can be thermally self-supported at the temperature range of 841 to 866 K. They also achieved at 700 W an energy conversion efficiency of 47% with fuel utilization of 75%. Finally, Funahashi et al. [16] also performed simulation studies for their series connected bundles of microtubular SOFCs. They concluded that the current collection method plays a crucial role as the total output power loss of the bundle was estimated to be 27.8%. They also suggested the use of porous MgO matrixes instead of LSCF, as magnesium oxide presents higher thermal conductivity.

The complete characterization of a microtubular SOFC stack must be solved taking into consideration the electric and also the thermal behavior of the complete system.

In the present paper the virtual work stack will be describe considering the electrical parameters and modeling the losses in each process. We will give the details of the thermal working in the simulation model and the critical parameters for the final design stack.

It will also describe the results of a first prototype 2-cell stack. The integration feasibility of the stack in a portable power module will be also demonstrated by the conceptual design of the system.

2. Materials and methods

2.1. Cell and stack fabrication

Anode supported microtubular cells used in this study were fabricated in a similar method as described in reference [17]. For the fabrication of the supporting tubes, NiO (Alfa-Aesar) was previously ball-milled in 2-propanol. The resulting NiO powder was mixed with pore former (corn-starch), 8YSZ (Tosoh) and acetone in order to achieve a final composition of 50vol% Ni and 50vol% YSZ. Then, tubes were fabricated by cold isostatic pressing (CIP) at 200MPa, and subsequently dried and presintered at 950ºC for 2 hours. As for the electrolyte, 8YSZ (Tosoh) was deposited by wet powder spraying (WPS) using 2-propanol as liquid vehicle. After drying, the tubes were cosintered at 1400ºC for 2hours. The final dimensions of the tubes were 2.4mm inner diameter and around 10-15cm length. A bilayer LSM (Fuelcell Materials)-YSZ (Tosoh) was finally used as cathode. Firstly, one functional layer of about 20µm (50vol%LSM - 50vol%YSZ) and then a current collector layer of about 20µm (80vol%LSM - 20vol%YSZ) were deposited by dip-coating and sintered at 1150ºC for 1.5 hours each step.

Nickel foam and platinum mesh (Goodfellow) were used for anode and cathode current collection, respectively. Platinum paste (Metalor) was also used to attach the mesh at the LSM-YSZ electrode.

Two analogue cells were used for the stack fabrication (Fig. 1). The cells were connected in series using Pt wires. The total active area of the cell was 8 cm^2. The cells were sealed into Macor® pieces which also acted as cell support.

Fig.1 Image of the 2-cell stack.

2.2. Electrochemical characterization

The electrochemical performance of the cells and the stack was tested at temperatures between 750 and 950 ºC, using humidified pure hydrogen (~3% H2O) as fuel (Q = 200 mls/min) and stagnant air as the oxidant. *j–V* (current density – voltage) curves were measured using an electronic charge (Servicio de Instrumentación Científica, Universidad de Zaragoza). Additional details regarding cell fabrication, microstructure of the cells and experimental setup for the electrochemical experiments can be found in references [17, 18, 19, 20].

2.3. Electrical characterization

From the electrical simulation model, an electrochemical losses analysis was done. In particular, the theoretical Nernst potential was calculated, taking into account the standard Nernst potential (E_0=0.977V) obtained for the experimental data; also oxygen, water and hydrogen partial pressures. The highest current through the cell, the highest losses there were; as a result the initial potential decreases. The activation, ohmic and diffusion losses were considered.

The activation losses are those associated with the energy needed to overcome electrochemical barriers in the reaction. The Bulter-Volmer equation (Equation 1) was considered.

$$\eta_{act} = \left(\frac{RT}{zFi_{oc}}\right)I \qquad (1)$$

where R is the ideal gasses constant, T is the temperature, z the number of electrons in the reaction, F the Faraday constant, i the density current, at least i_{oc} the limiting interchange current which values were obtained interpolating experimental data at different temperatures.

Related to the ions difficulty to pass through the membrane also the work required to perform this operation are the ohmic losses expressed by the equation 2.

$$\eta_{ohm} = R_{ohm}I \qquad (2)$$

The $\mathbf{R_{ohm}}$ value also was obtained from experimental data of R_0 at a determinate temperature. The resistance temperature dependence was modelled by an Arrhenius law (Equation 3).

$$R_{ohm} = R_o exp\left(\frac{E_o}{TK}\right) \qquad (3)$$

At least, associated with the concentration gradients that occurs in the vicinity of the membrane where the hydrogen consumption is very high, are the diffusion losses. For an anode-supported cell, are expressed by equation 4.

$$\eta_{conc} = -\left(\frac{RT}{2F}\right)\left[ln\left(1-\left(\frac{i}{i_{as}}\right)\right)+ln\left(1+\left(\frac{ip^{a}_{H_2}}{i_{as}p^{a}_{H_2O}}\right)\right)\right] \quad (4)$$

where R is the ideal gasses constant, T is the temperature in Kelvin, F the Faraday constant, i the current per surface unit, *p* the partial pressure of each element and i_{as} the limiting current through the mea (membrane electrode assembly), which was obtained by the expression 5.

$$i_{as} = \left(\frac{2Fp_{H_2}D_{a(eff)}}{RTl_a}\right) \quad (5)$$

where l_a is the anode thickness and $D_{a(eff)}$ the effective anode diffusion coefficient; obtained by equation 6.

$$D_{12} = D_{a(eff)} = \left(\frac{0.00186T^{\frac{3}{2}}\left(\frac{1}{M_1}+\frac{1}{M_2}\right)^{\frac{1}{2}}}{\rho\sigma_{12}^{2}\Omega}\right) \quad (6)$$

where M_1 and M_2 are the two in contact species molecular weight and T is the temperature in Kelvin. Knowing the coefficient for one temperature, other coefficients were obtained considering the denominator as a joined constant.

2.4. Thermal characterization

The integration feasibility of the stack in a portable power module was also demonstrated by the conceptual design of the system. This system includes a burner and heat exchanger to warm up the stack up to 900ºC using the exhaust hydrogen non utilized by the cells. It can be operated in two different modes; the first one will be a warm up mode for heating all the system until it reaches the operation temperature. The second one will be the electric power delivery, controlling and stabilizing the working temperature.

A thermal energy balance of the system was simulated using Matlab Simulink ®. The operation modes of the system, efficiency and convection inside the stack were studied via the Simulink® simulation. The diagram block is shown in fig. 2.

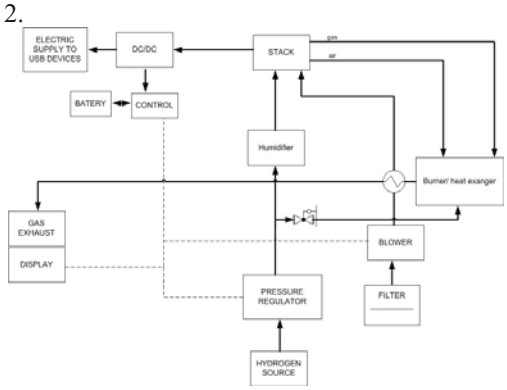

Fig. 2 Diagram block for the Simulink® simulation.

During the heating operation mode, the fuel sets on fire at the burner and warm up the air from the blower. The air circulated through the stack increased the temperature up to the operation setpoint. At the power delivery mode, part of the hydrogen will flow through the humidifier and will get into the stack. Part of the fuel will also be burned with the output gasses interchanging the residual heat and as a consequence the temperature will be balanced.

The main energy losses sources will be analyzed. For this purpose, three devices will be simulated: the microtubular cells stack, ideal burner and heat exchanger. Firstly, the mass and energy balance in the stack was implemented, considering all energy exchanges that take place with the external environment. The different flows and energy sources considered at the energy balance were:

- Fuel mass and fuel energy (heat capacity, C_p).
- Air mass and its temperature.
- Output gasses mass flow and output temperatures.
- Internal stack heat generated.
- Heat losses at the box sides.

Considering the insulator thickness (10cm), its conductivity ($0.044 Wm^{-1}K^{-1}$, rockwool) and also its external ($10 Wm^{-2}K^{-1}$) and internal convection rate which was modified from $100 Wm^{-2}K^{-1}$ to $0.01 Wm^{-2}K^{-1}$ in order to analyze the losses dependence in the system. As a result of this model the following parameters were obtained.

- Output flow: temperature, mass flow and fuel concentration.
- Electric efficiency.
- Heat efficiency.
- Stoichiometric rate.
- Lost heat at the box sides.

The burner took an input fuel flow and calculated the output flow temperature considering all the fuel in the flow burns and also all the generated heat was transformed into an increasing flow temperature. Thus, the fuel heat capacity ($3.4 KcalKg^{-1}K^{-1}$) and the fuel lower heating value (LHV) ($28788 KcalKg^{-1}$)

were needed. Two gas flows, with its corresponding temperatures, reached the heat exchanger. The interchange heat between both gases considered the heat exchanger efficiency (1 in this case) for the calculation. The model also postulated the same heat capacity for both gases as the air (0.24 $KcalKg^{-1}$). Eventually the system reached 50W electrical production and the complete balance of plant and stack calculations gave an overall electrical efficiency around 40% with 70W of losses.

3. Results and Discussion

3.1. Electrochemical characterization of the single cells

Analogue cells were extensively characterized as a function of the temperature, fuel utilization and gas composition in references [17, 18, 20]. The purpose of this study was to find cells presenting similar performance to be used for the stack fabrication. In fig. 3 we show typical results for one of the single cells, which are consistent with previously reported data [17]. For example, at 895ºC, using pure RT humidified hydrogen (~3%H2O) as fuel at the anode side and stagnant air at the cathode side, current densities of about $600mWcm^{-2}$ were obtained for both of the cells of the stack.

3.2. Electrochemical characterization of the 2-cell stack

A two-cell stack prototype was fabricated in order to proof the scalability of the cells. Each cell presented an active area of $4cm^2$ and as a consequence the total active area of the stack was $8cm^2$. The stack was characterized at a temperature of 800ºC, as shown in fig. 4. At this temperature, an OCV of 2.04 V was measured, a value slightly lower that the predicted from the Nernst equation (2.2V). This difference could be attributed to small gas leakages through the YSZ electrolyte layer of the cells. In fig. 4, we can also observe a maximum power output of about 0.9W at an operation voltage of 1.1V. Several losses were clearly observed in comparison with the single cell results, especially those associated with current collection at the cathode side, interconnection between cells and gas distribution at the anode side. Note that this is a preliminary result and it will serve as a first approach for further development of the experimental stack fabrication.

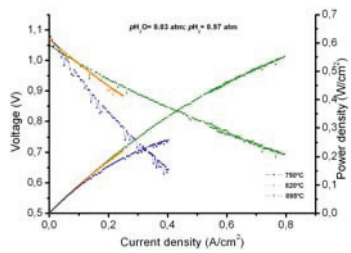

Fig. 3 Polarization curve for one cell of the 2-cell stack.

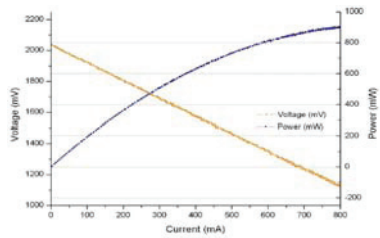

Fig.4 Polarization curve of the 2-cell stack.

3.3. Electric simulation

For the complete cell characterization two simulation models were done. The first one, for the electrical characterization; the second, for the thermal behavior. A model for the complete electric cell characterization was developed and all the constants and parameters were obtained (Table 1), The polarization curve was obtained for 600, 700, 800 and 900ºC and also for 5, 15, 30, 90% fuel concentration. Fig. 5a show the polarization curve for 800ºC and a fuel concentration of 90% also the different losses are included. It was showed a strong dependence on the temperature with a maximum power of 553mW for 800ºC between the value of 767mW for 900ºC both for a fuel concentration of 99% and 735mW for 90% fuel concentration and 534mW for 30% concentration at a temperature of 900ºC (Fig. 5b and 5c).

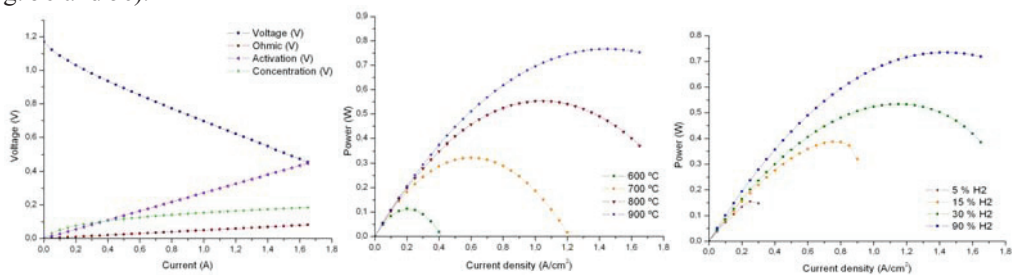

Fig.5. (a) Theoretical polarization curve for one single cell (b) Power curves and its temperature dependence (c) Power curves and its fuel concentration dependence.

Table 1. Variables for the complete cell characterization.

Variable	Value	Units
E^o (800ºC)	0.97	V
R	8.31	$JK^{-1}mol^{-1}$
n	2	-
F	964851.33	$Cmol^{-1}$
z	2	-
i_{oc} (800ºC)	132	$mAcm^{-2}$
E_o	$1.376e^{-19}$	J
R_o	0.00001	$Ohmcm^2$
l_a	0.00002	M
M_1	2	-
M_2	18	-

$D_{a(eff)}$(800ºC)	0.054	m^2s^{-1}
i_{as}(800ºC)	57969.51	Am^{-2}
C= $\rho\ \sigma_{12}{}^{2}\Omega$	900	-

With this model the experimental and theoretical data were compared. The tested parameters were predicted and the cells could be operated at the optimum condition.

3.4. Thermal simulation

From the thermal simulation model three are the main factors that had been taking into account; convection coefficient, layer temperature and exchanger efficiency. It was shown that the most limitation factor for the efficiency was the isolation of the stack. In case the stack is not isolated properly, most of the hydrogen will be used to maintain the stack temperature, decreasing the overall system efficiency. As it is showed in figure 6a, the convection rate it is not a limiting factor as in most of the cases the model presented high losses. The coefficient was tested from $100Wm^{-2}K^{-1}$ to $0.01Wm^{-2}K^{-1}$ at a temperature of 1173K, only if both convection coefficients are lower than $1Wm^{-2}K^{-1}$ they will be limiting factor as the losses (51W) would equal the input heat (50W), and therefore would not need the heat of the afterburner. In addition, the power losses increase linearly with the layer boundary temperature (See fig. 6b) for the same internal and external convection rate value. Tested these coefficients at $10Wm^{-2}K^{-1}$, the limiting temperature was 900K (627ºC), where the losses were 48.69W.

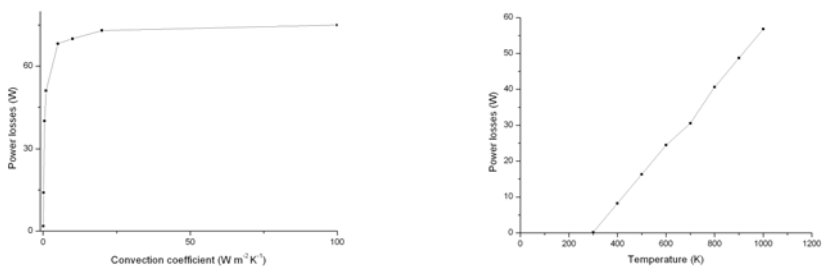

Fig.6. (a) Power losses as a function of convection rate (b) Power losses as a function of temperature.

Furthermore, the losses at the exchanger output were analyzed. The heat power losses at the layer were considered null, besides fuel utilization was always close to 1 and the temperature to 1173K, thus the gasses losses was the only one. A fixed value of $1.05e^{-6}kgs^{-1}$ fuel flow was considered so different stoichiometric coefficients were analyzed taking into consideration an exchanger efficiency of 0.8, 0.6, 0.4, 0.2. It was showed that stoichiometric coefficient of 1 was needed at least for complete fuel cell refrigeration. This means the exchanger losses were not the most important of the system, in absence of wall losses, the temperature in the stack could be maintained without an afterburner.

As it was showed, the most critical factor was the wall isolation and its losses, instead of the extremely optimization of the exchanger efficiency.

3.5. 3D Model

A modular 3D design of the stack is also drawn using Solid Works®. This model is used for the study of possible flow paths through the stack (Fig. 7). The model was designed taking into account the mechanical stability and the thermal expansions in an autonomous portable power unit 3D design complying with usual product specifications.

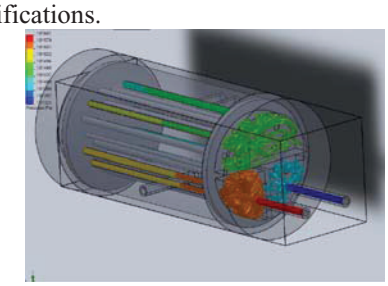

Fig.7 Stack flow paths design.

In this design, 16 cells of 15cm long are integrated in a stack structure module. The physical active area of those cells would be 8cm2, and according with the experimental results each cell should produce 3,125W, as a consequence, the full stack would produce around 50Watts. The model is oversized assuming a low current density to ensure at least 50W production and longer durability. It was also considered a four times recirculation design, anode combustion for warm up and internal heat exchanging. This actual 3D stack model is a design exercise, however it will be modified to fit the requirements defined in future experiments with real single cells and stacks.

A prototype model was also defined for the complete integration of the components. As it is shown in Fig.8 the heat exchanger as well as the stack are joined together so that the heat can be retained, decreasing the global losses.

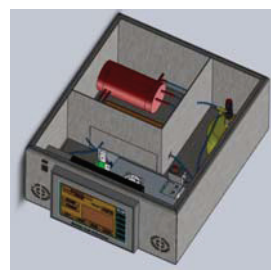

Fig.8 Stack design.

4. Conclusions

Ni-YSZ/YSZ/YSZ-LSM anode-supported microtubular fuel cells have been successfully manufactured and characterized. Different temperatures have been tested obtaining about 600 $mWcm^{-2}$ at 895ºC using pure humidified hydrogen as fuel. In addition, a 2-cells stack prototype has been fabricated in order to prove its scalability.

Electric and thermal model were development. The system showed highly strong dependence on temperature and also on fuel concentration related to final produced power generating 553mW for 800ºC between the value of 767mW for 900ºC.

The complete system has been simulated using Matlab Simulink®. For an electric power of 50W the system had an efficiency around 40% with 70W of losses. Besides, the results showed the internal

convection rate is not a critical factor as it was lower than $1Wm^{-2}K^{-1}$ however the device isolation was a critical factor in maintaining the stack temperature instead of the exchanger efficiency.

In addition, a 3D design of the stack of the complete device has been drawn with Solid Works®

Acknowledgments

We would like to thank grants MAT2009-14324-C02-01, MAT2009-14324-C02-02 and EVIDOS, financed by the Spanish Government and Feder program of the European Community for funding the project.

References

[1] S.C.Singhal y K.Kendall, «High Temperature Solid Oxide Fuel Cells. Fundamentals, design and applications.,» Elsevier, Oxford, 2003.

[2] K.S.Howe, G.J.Thompson y K.Kendall, «Micro-tubular solid oxide fuel cells and stacks,» Journal of Power Sources, vol. 196, pp. 1677-1686, 2011.

[3] K.Kendall, «Progress un Microtubular Solid Oxide Fuel Cells.,» International Journal of Applied Ceramic Technology, vol. 7, pp. 1-9, 2010.

[4] T.Suzuki, Z.Hasan, Y.Funahashi, T. Yamaguchi, Y.Fujishiro y M.Awano, «Impact of Anode Microstructure on Solid Oxide Fuel Cells,» Science, vol. 325, pp. 852-855, 2009.

[5] K.W.Galloway y M.Sammes, «Performance degradation of microtubular SOFCs operating in intermediate temperature range,» Journal of Electrochemical Society, vol. 156, pp. B526-B531, 2009.

[6] V.Lawlor, S.Griesser, G.Buchinger, A.G.Olabi, S.Cordiner y D. Meissner, «Review of the micro-tubular solid oxide fuel cell Part.I Stack design issues and research activities,» Journal of Power Sources, vol. 193, pp. 387-399, 2009.

[7] M. Othman, N.Droushitotis, Z.Wu, G.Kelsall y K.Li, «High-performance, anode-supported, microtubular SOFC prepared from single-step-fabricated, dual-layer hollow fibers,» Advanced Materials, vol. 21, pp. 2480-2483, 2011.

[8] W.Bujalski, C.M.Dickwal y K.Kendall, «Cycling of three solid oxide fuel cell types,» Journal of Power Sources, vol. 171, pp. 96-100, 2007.

[9] T.Suzuki, T.Yamaguchi, Y.Fujishiro y M.Awano, «Improvement of SOFC performance using a microtubular anode-supported SOFC,» Journal of Electrochemical Society, vol. 153, A925-A928 2006.

[10] T.Yamaguchi, K.V.Galloway, J.Yoon y N.M.Sammes, «Electrochemical characterizations of microtubular solid oxide fuel cells under a long-term testing at intermediate temperature operation,» Journal of Power Sources, vol. 196, pp. 2627-2630, 2011.

[11] Y.H.Heo, J.W.Lee, S.B.Lee, T.H.Lim, S. Park, R.H.Song, C.O.Park y D.R.Shin, «Redox-induced performance degradation of anode-supported tubular solid oxide fuel cells,» International Journal of Hydrogen Energy, vol. 36, pp. 797-804, 2011.

[12] G. F.Calise y N.Sammes, «Experimental analysis of performance degradation of micro-tubular solid oxide fuel cells fed by different fuel mixtures,» Journal of Power Sources, vol. 196, pp. 301-312, 2011.

[13] Y.Du, C.Finnerty y J.Jiang, «Thermal stability of portable microtubular SOFCs and stacks,» Journal of Electrochemical Society, vol. 155, pp. B972-B977, 2008.

[14] M.Lockett, M. Simmons y K.Kendall, «CFD to predict temperature profile for scale up of micro-tubular SOFC stacks,» Journal of Power Sources, vol. 131, pp. 243-246, 2004.

[15] N.Watanabe, T.Ooe y T.Ishihara, «Design of thermal self supported 700W class, solid oxide fuel cell module using LSGM thin film micro tubular cells,» Journal of Power Sources, vol. 199, pp. 177-123, 2012.

[16] Y.Funahashi, T.Shimamori, T.Suzuki, Y.Fujishiro y M.Awano, «Simulation study for the optimization of microtubular solid oxide fuel cell bundles,» Journal of Fuel Cell Science and Technology, vol. 11, pp. 116-123, 2011.

[17] M.A.Laguna-Bercero, R.Campana, A.Larrea, J.A.Kilner y V.M.Orera, «Performance and anging of microtubular YSZ-based solid oxide regenerative fuel cells,» Fuel Cell, vol. 11, pp. 116-123, 2011.

[18] R.Campana, R.I.Merino, A.Larrea, I.Villarreal y V.M.Orera, «Fabrication, electrochemical characterization and thermal cycling of anode supported microtubular solid oxide fuel cells,» Journal of Power Sources, vol. 192, pp. 120-125, 2009.

[19] M.A.Laguna-Bercero, R.Campana, A.Larrea, J.A.Kilner y V.M.Orera, «Steam electrolysis using a microtubular solid oxide fuel cell,» Journal of Electrochemial Society, vol. 157, pp. B852-B855, 2010.

[20] R.Campana, A.Larrea, R.I.Merino, I.Villarreal y V.M.Orera, «SOFC mini-tubulares basadas en YSZ,» Boletín de la Sociedad Española de Cerámica y Vidrio, vol. 47, pp. 7-12, 2008.